Original Research Article

JABFM Journal of Applied Biomaterials & Functional Materials

Cumulative antitumor effect of bismuth lipophilic nanoparticles and cetylpyridinium chloride in inhibiting the growth of lung cancer

Journal of Applied Biomaterials & Functional Materials
1–10

DOI: 10.1177/22808000231161177
journals.sagepub.com/home/jbf
SAGE

Claudia María García-Cuellar[1], Rene Hernández-Delgadillo[2], Jesús Alejandro Torres-Betancourt[2], Juan Manuel Solis-Soto[2], Irene Meester[3], Yesennia Sánchez-Pérez[1], Nayely Pineda-Aguilar[4], Sergio Eduardo Nakagoshi-Cepeda[2], Rosa Isela Sánchez-Nájera[2], María Argelia Akemi Nakagoshi-Cepeda[2], Shankararaman Chellam[5] and Claudio Cabral-Romero[2]

Abstract

Objective: To determine the combined antitumor effect of bismuth lipophilic nanoparticles (BisBAL NP) and cetylpyridinium chloride (CPC) on human lung tumor cells.

Material and methods: The human lung tumor cells A549 were exposed to 1–100 µM BisBAL NP or CPC, either separately or in a 1:1 combination. Cell viability was measured with the PrestoBlue assay, the LIVE/DEAD assay, and fluorescence microscopy. The integrity and morphology of cellular microtubules were analyzed by immunofluorescence.

Results: A 24-h exposure to 1 µM solutions reduced A549 growth with 21.5% for BisBAL NP, 70.5% for CPC, and 92.4% for the combination ($p < 0.0001$), while a 50 µM BisBAL NP/CPC mixture inhibited cell growth with 99% ($p < 0.0001$). BisBAL NP-curcumin conjugates were internalized within 30 min of exposure and could be traced within the nucleus of tumor cells within 2 h. BisBAL NP, but not CPC, interfered with microtubule organization, thus interrupting cell replication, similar to the action mechanism of docetaxel.

Conclusion: The growth inhibition of A549 human tumor cells by BisBAL NP and CPC was cumulative as of 1 µM. The BisBAL NP/CPC combination may constitute an innovative and cost-effective alternative for treating human lung cancer.

Keywords

Cumulative antitumor effect, bismuth lipophilic nanoparticles, cetylpyridinium chloride, human lung cancer, chemotherapy, uptake assays

Date received: 15 July 2022; revised: 3 February 2022; accepted: 14 February 2023

[1]Subdirección de Investigación Básica, Instituto Nacional de Cancerología, Ciudad de México, México
[2]Laboratorio de Biología Molecular, Facultad de Odontología, Universidad Autónoma de Nuevo León, UANL, Monterrey, Nuevo León, México
[3]Departamento de Ciencias Básicas, Universidad de Monterrey, San Pedro Garza García, México
[4]Centro de Investigación en Materiales Avanzados, S.C. (CIMAV), Unidad Monterrey, Nuevo León, México
[5]Texas A&M University, College Station, TX, USA

Corresponding author:
Claudio Cabral-Romero, Laboratorio de Biología Molecular, Facultad de Odontología, Universidad Autónoma de Nuevo León, UANL, Dr. E. Aguirre Pequeño and Silao s/n., Mitras centro, Monterrey, Nuevo León C.P.64460, México.
Email: claudio.cabralrm@uanl.edu.mx

Introduction

Lung cancer (LC) continues to be a major issue in modern medicine.[1] In 2020, LC was the second most common type of cancer worldwide and the leading cause of cancer-related deaths, accounting 1.8 million deaths or 18% of all cancer-related deaths.[2,3] In Mexico, from 2012 to 2016, LC was responsible for the highest mortality, with 33,781 deaths.[4] LC is more prevalent in Mexican men (gender ratio: 1.6:1) and its mortality rate is higher among older people and in urban areas.[4] In addition to the well-established association with cigarette smoking,[5] exposure to wood smoke[6] and polluted air[7] is also an important risk factor for LC in Mexico. Unfortunately, LC is often diagnosed at advanced stages, which is strongly associated with higher mortality.[8] Surgery is the first treatment option for LC patients, followed by radiotherapy and chemotherapy. Drugs like doxorubicin and mitomycin are obsolete and no longer used[9–11] while crizotinib, erlotinib, and gefitinib are more commonly used today.[12–14] Research for new treatments continues in order to improve efficacy, reduce adverse side-effects, and lower cost. Nanomedicine is a new discipline that offers novel anticancer approaches, including target-specific drug delivery for higher efficacy and biocompatibility.[12] Nanomedicine proposals seek synergistic effects of nanomaterials and conventional anticancer agents. One example is the combination of cisplatin and an EGFR-targeting nanovehicle containing anti-Bcl-xL siRNA.[15] Another example are docetaxel-loaded nanomicelles, which induced apoptosis in Lewis LC cells, as shown in an in vitro study.[16] We have reported on the anticancer properties of bismuth lipophilic nanoparticles (BisBAL NP) on human breast, cervicouterine, prostate, and colorectal cancer cells.[17–19] However, BisBAL NP have not been tested on human LC.

Cetylpyridinium chloride (CPC) has antimicrobial properties and is used in mouthwashes and oral care products.[20] Importantly, CPC has also been shown to inhibit glioblastoma cell growth in a dose-dependent manner.[21] The anticancer potential of CPC on various human tumor cells has been understudied. CPC has been found to inhibit the growth of human breast cancer cells non-selectively.[22] Previously, CPC was reported to be highly cytotoxic to human LC cells (A549 cells) with an IC_{50} value of 5.79 µg/mL.[23]

The current study describes the cumulative effect of BisBAL NP and CPC on the growth inhibition and cytotoxicity of human LC A549 cells. A mixture of BisBAL NP and CPC at a 1:1 ratio at 50 µM inhibited A549 cell growth by 99% ($p < 0.0001$). The mechanism of action mechanism seems to be that BisBAL NP alter the microtubule network, which affects cell replication in a way similar to docetaxel. The here reported results confirm our previous findings on the selective susceptibility of tumor cells to BisBAL NP, which seems to be reinforced by CPC.

Material and methods

Synthesis and characterization of bismuth nanostructures

BisBAL NP were synthesized using the colloidal method.[24] All chemical reagents used in this study were of analytical grade and purchased from Sigma-Aldrich (Sigma-Aldrich; St. Louis, MO). Briefly, bismuth nitrate was dissolved in propylene glycol and heated to 80°C for 2 h. Next, it was mixed with 2,3-dimercapto-1-propanol in a 2:1 molar ratio and reduced by 75 mM sodium borohydride under continuous mixing. A stock batch of 25 mM BisBAL NP was stored at room temperature and further diluted in culture medium to generate µM concentrations. To characterize BisBAL NP (morphology, diameter, and distribution), a scanning electron microscope (SEM; FEI Tecnai G2 Twin, Hillsboro, OR) was employed at 160 kV accelerating voltage. The chemical composition of BisBAL NP was analyzed by energy dispersive-SEM.[18] The UV-Vis spectrum of a BisBAL NP solution was recorded using a spectrophotometer (SpectraMax Plus 384Abosorbance Microplate Reader, Molecular Devices, LLC, Sunnyvale, CA).[17]

BisBAL NP/CPC solution

A 1 mM sterile stock solution of CPC (Sigma-Aldrich; St. Louis, MO) in bidistilled water was diluted in culture medium to the desired final concentrations of 1, 5, 10, 50, and 100 µM, just before the experiment and mixed 1:1 with a BisBAL NP suspension when needed.

Cell culture and drug exposure

The human LC cell line A549 (ATCC, CCL-185; ATCC, Rockville, MD, USA) and the non-tumor human lung fibroblast cell line LL47 (MaDo) (ATCC CCL-135) were grown in DMEM/Ham's F12 (DMEM/F12) culture medium supplemented with 10% fetal bovine serum (Gibco-Invitrogen, Carlsbad, California, USA), 100 U/mL penicillin, 100 µg/mL streptomycin, and 0.25 µg/mL amphotericin B (Sigma-Aldrich; St. Louis, MO) at 37°C and 5% CO_2, as described previously.[18] Confluent monolayers were detached with trypsin (Gibco-Invitrogen, Carlsbad, California, USA) and washed with 10 mM phosphate buffer saline, pH 7.3 (PBS) at 500×*g*. For drug exposure, A549 cells (1×10^5/well; 96-well plate) or LL47 control cells were incubated with CPC at final concentrations of 100, 50, 10, 5, 1, or 0 µM; BisBAL NP at final concentrations of 100, 50, 10, 5, 1, or 0 µM, or a combination at a 1:1 ratio. Incubations with 500 µM doxorubicin (DOX) (Doxolem, Teva Lab, Madrid, Spain) or 500 µM docetaxel (DTXZurich Pharma, Mexico City, Mexico) served as positive controls of growth inhibition, while drug-free cell cultures were employed as growth controls.

Cell viability, IC_{50} value, selectivity index, and cytotoxicity assays

To evaluate cell viability, the PrestoBlue assay (Life Technologies Corporation, Oregon, USA) was used according to the manufacturer's instructions.[25,26] Absorbance at 570/600 nm was measured with a microplate reader (Biotek, Winooski, Vermont, USA). Viability was expressed as a percentage of the growth control. For IC_{50} determination, A549 and LL47 cells were exposed for 24 h to BisBAL NP/CPC series (0.1, 0.375, 0.75, 1.5, 3, 6.25, 12.5, 25, and 50 μM). The selectivity index (SI) of BisBAL NP/CPC was calculated as follows: IC_{50} for no-tumoral cell line LL447/IC_{50} for A549 cells. An SI >1 is considered favorable as it indicates a higher drug efficacy against tumor cells than no-tumor cells. Studies were done in triplicate.

The cytotoxicity of A549 cells exposed to CPC or BisBAL NP was evaluated with a Live/Dead kit (Molecular Probes Inc, OR, USA). Briefly, A549 cells were exposed to 5 μM CPC, 5 μM BisBAL NP, or the 1:1 combination, for 24 h. After drug removal and washing with PBS, cells were stained with calcein AM/ethidium homodimer-1 in 100 μL following the instructions of the manufacturer. Fluorescent cells were observed with an EVOS cell imaging system (Thermo Fisher Scientific, CA, USA).

Cellular uptake of BisBAL NP

To quantify cellular BisBAL NP uptake, BisBAL NP was labeled with curcumin (Cur), which has intrinsic fluorescence properties. Hereto, 4 μL of a 1 mM curcumin (Sigma-Aldrich) solution in dimethyl sulfoxide was mixed with 996 μL 100–250 μM BisBAL NP.[27] The suspension of BisBAL NP-Cur was freshly prepared when needed. A549 cells (1×10^4 in 100 μL supplemented culture medium) on sterile 8-well chamber slides (Lab-tekk II, Thermo Fisher Scientific, NY, USA) were exposed to 250 μM BisBAL NP-Cur for 30–120 min (37°C, in the dark) and washed three times with PBS. Nuclei were counterstained with DAPI (1 mg/mL). Fluorescent cells were observed with an EVOS cell imaging system using FITC and DAPI filters (Thermo Fisher Scientific, CA, USA).

Microtubule network immunofluorescence

The microtubule network was studied as a possible intracellular target of BisBAL NP. A549 cells were exposed for 24 h to BisBAL NP, 10 μM CPC, or the 1:1 combination, as well as to the DTX control as described above. After washing, cells were fixed with 100% methanol for 5 min, permeabilized with 0.5% Triton X-100 in PBS for 30 min, and blocked with 3% bovine serum albumin in PBS for 30 min at room temperature. After a triple wash with cold PBS, A549 cells were exposed to Alexa Fluor® 488-conjutated anti-tubulin antibody (AB-197737; Abcam, Cambridge, UK) at 1:200 in PBS for 18 h at 4°C in the dark. After another triple wash with cold PBS, nuclei were counterstained with DAPI. Coverslips were mounted with glycerin. Fluorescent cells were observed with a confocal microscope (Zeiss LSM 7 Duo; Carl Zeiss; Germany).

Statistical analysis

Tests were performed in triplicate. One-way ANOVA was employed to analyze data among groups. A significance level of $\alpha = 0.05$ was considered.

Results

Characterization of BisBAL NPs by SEM

BisBAL NP synthesis with the colloidal method yielded spherical nanoparticles with an average size of 29.15 ± 7.05 nm, which formed electron-dense conglomerates (Figure 1(a) and (b)). The EDX spectrum proved that the nanoparticles contained bismuth (Figure 1(c)). The UV-visible absorbance spectrum confirmed that the bismuth nanoparticles have affinity for 1-octanol,[24] characteristic associated to dithiols groups on NP surface (Figure 1(d)).

Antitumor effect of CPC, BisBAL NP, or mixture BisBAL NP/CPC

A549 growth inhibition was evident as of 1 μM BisBAL NP (21.5%) and 1 μM CPC (70.5%), while the combination had a cumulative impact: 92.4% growth inhibition ($p < 0.0001$) (Figure 2). In contrast, the positive control of growth inhibition (DOX; 500 μM) inhibited only 76% after a 24-h exposure ($p < 0.0001$) (Figure 2). Growth inhibition was stable for CPC, but dose dependent for BisBAL NP. As a result, the 1:1 combination of BisBAL NP and CPC at 50 and 100 μM yielded growth inhibitions of 99% and 100%, respectively ($p < 0.0001$) (Figure 2). Altogether, these results suggest a cumulative effect of BisBAL NP/CPC-induced growth inhibition of tumor cells.

LIVE/DEAD assays

A Live/Dead test was used to analyze cell cytotoxicity after a 24-h exposure to 10 μM CPC, 10 μM BisBAL NP, or the 1:1 BisBAL NP/CPC mixture. Live/Dead assays confirmed the pattern of PrestoBlue assays: the BisBAL NP/CPC mixture induced a larger number of dead cells (red stain) than each substance separately and was almost identical to the positive control of cytotoxicity, 500 μM DOX (Figure 3).

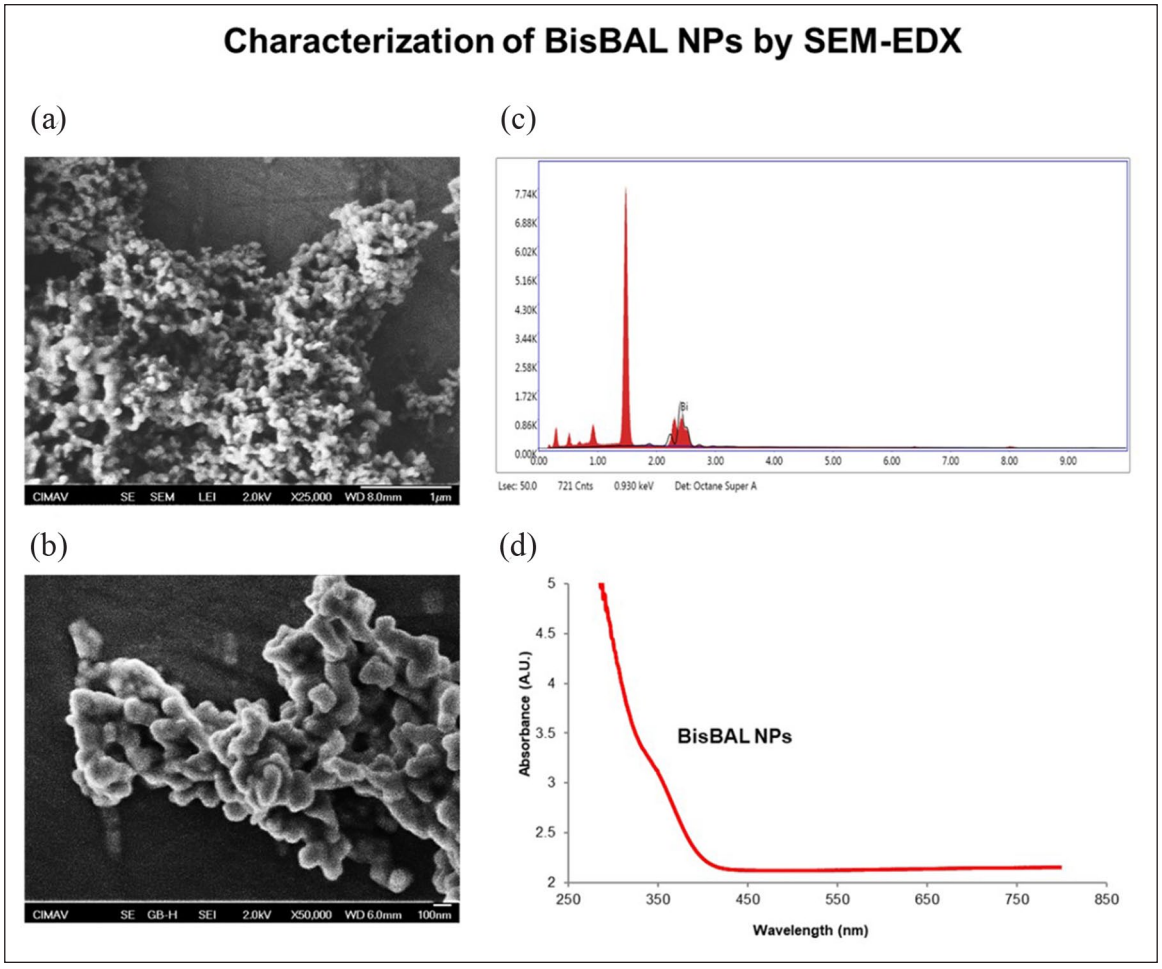

Figure 1. Characterization of BisBAL NP: (a and b) scanning electron microscopy (SEM) images of BisBAL NP, (c) the chemical elemental map was obtained by energy-dispersive X-ray spectroscopy (EDX), and (d) the UV-visible absorbance spectrum of BisBAL NP.

IC_{50} assays and selectivity index

A 24-h exposure to a BisBAL NP/CPC concentration series revealed that the IC_{50} value for A549 cells was 0.9 µM (Figure 4). In contrast, the IC_{50} of BisBAL NP/CPC on LL47 (MaDo) cells was 2.7 µM (Figure 4). Thus, cancer cells were more susceptible to BisBAL NP/CPC than normal healthy cells and the IC_{50} values confirm the antitumor efficacy of BisBAL NP/CPC on A549 cells (Figure 2). The SI for BisBAL NP/CPC was 3 (Figure 2), which indicates a favorable SI.

Cellular uptake of BisBAL NP

To verify BisBAL NP entry into tumor cells, BisBAL NP-Cur destiny was observed by fluorescence microscopy after a 2-h exposure to 250 µM Bisabol NP-Cur. In contrast to cells exposed to curcumin alone, A549 cells exposed to BisBAL NP-Cur became fluorescent, indicative of BisBAL NP-Cur entry (Figure 5(a)). BisBAL NP-Cur fluorescence was quantified and compared against curcumin alone (Figure 5(b)). Curcumin proved to be a useful label to track BisBAL NP within tumor cells. Interestingly, BisBAL NP-Cur fluorescence was strongest within nuclei (Figure 5(c)). A more detailed evaluation of BisBAL NP-Cur localization and its effect on A549 cell viability was conducted at 30-, 60-, and 120-min of exposure to 100 µM BisBAL NP. The results revealed a time-dependent increase in green fluorescence, indicating BisBAL NP-Cur internalization and growth inhibition (Figure 6). After a 30-min exposure to BisBAL NP-Cur, A549 cells displayed faint green fluorescence and 66% growth inhibition. After a 120-min exposure, A549 cells were strongly fluorescent, and the growth inhibition was 87% (Figure 6(a) and (b)). Altogether, these results suggest a quick internalization of BisBAL NP into tumor cells accompanied by growth inhibition within a relatively short time of 2 h.

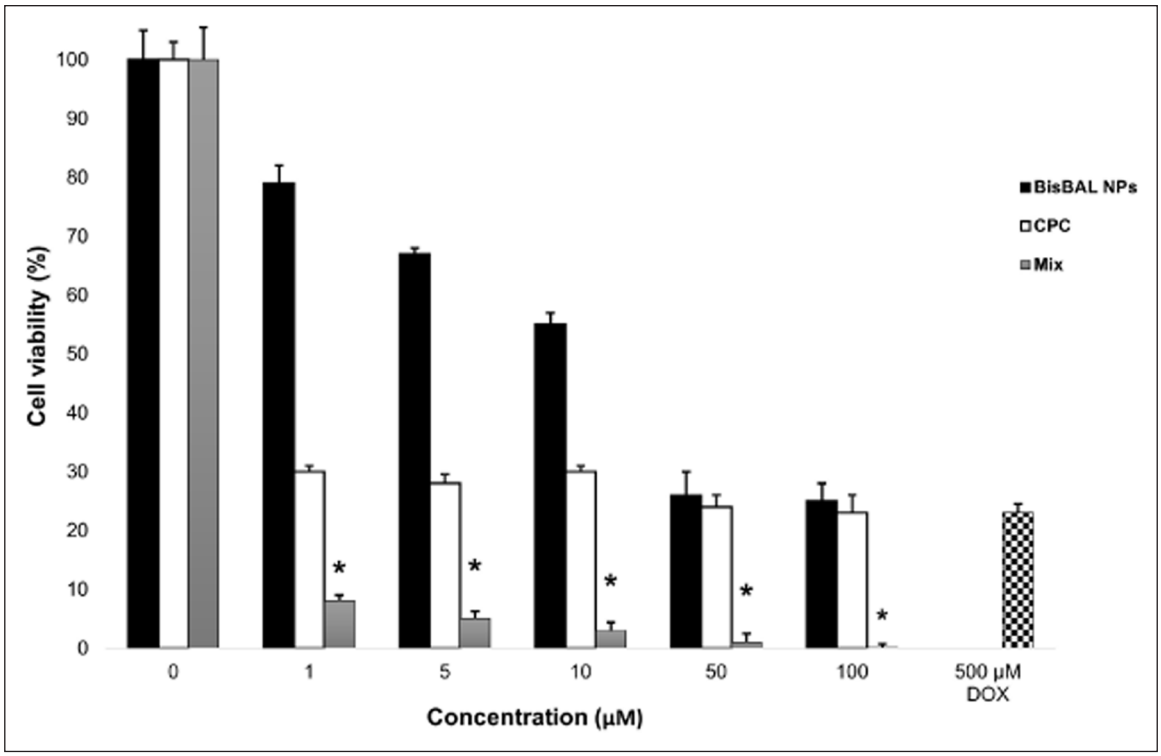

Figure 2. Cumulative antitumor effect of BisBAL NP/CPC on human lung cancer cells. The percentage of cell viability of A549 cells after a 24-h exposure to CPC, BisBAL NP, or a 1:1 combination at various concentrations (1–100 µM) was obtained by PrestoBlue assays; 500 µM doxorubicin (DOX) served as a positive control of growth inhibition, while drug-free cell cultures served as growth controls. After a one-way ANOVA with Tukey's HSD Test, all samples were significantly different ($p < 0.0001$), except for 50 µM BisBAL NP versus 50 µM CPC and 100 µM BisBAL NP versus 100 µM CPC. Asterisks indicate a significant statistical difference among groups. Bars indicate mean ± SD.

Microtubule network immunofluorescence

To evaluate whether CPC, BisBAL NP, or the BisBAL NP/CPC mixture could damage the cytoskeleton after cell entry, the integrity and morphology of the microtubule network were analyzed by immunocytofluorescence. After a 24-h exposure to 10 µM BisBAL NP, the typical filamentous distribution of microtubules changed into a granular appearance, accompanied by the rounding-up of previously extended cells and the formation of conglomerates (Figure 7). The same was observed after a 24-h exposure to the 1:1 BisBAL NP/CPC mixture, but exposure to 10 µM CPC did not alter the typical microtubule morphology. The positive control of growth inhibition, DTX, which is known for interfering with microtubule organization, affected microtubule organization and cellular morphology and aggregation in a way that was very similar to exposure to BisBAL NP (Figure 7). In summary, BisBAL NP and DTX interfere with the microtubule network of tumor cells.

Discussion

There is a growing interest to combine chemosensitizers and cytostatics to overcome resistance to cancer treatment.[28] So far, few studies have evaluated the anti-tumor effect of combinations of anti-tumor nanostructures and other anti-tumor molecules. Therefore, we investigated the anti-tumor potential of the combination of BisBAL NP and CPC against human LC cells. In this work it was found that BisBAL NPs and CPC inhibited A549 cell growth separately as of 1 µM. Recently, it has been reported that zinc-doped copper iron oxide nanoparticles inhibited A549 cell growth with an IC_{50} of 95.8 µg/mL.[29] Skóra et al.[30] reported that silver nanoparticles within liposomes, which were labeled with epidermal growth factor, reduced the metabolic activity of A549 cells and had antitumor activity. In our study, A549 cell growth inhibition due to BisBAL NP and CPC was cumulative and probably mediated by different mechanisms as only BisBAL NP affected microtubule organization, but CPC not. Currently, combination treatment to obtain higher efficacy is a popular strategy to treat LC patients.[31] The combination of amlodipine with the novel anticancer drug gefitinib reduced A549 proliferation by altering the cell cycle.[32] Also, doxorubicin-loaded iron oxide nanoparticles generated excellent results against glioblastoma.[33] In our study, the 1:1 mixture of 10 µM NP/CPC mixture promoted cell death as evidenced with the LIVE/DEAD assays. The IC_{50} value of BisBAL/CPC was 0.9 µM on A549 cells and 2.7 µM on LL47 (MaDo) cells, suggesting that tumor cells are more

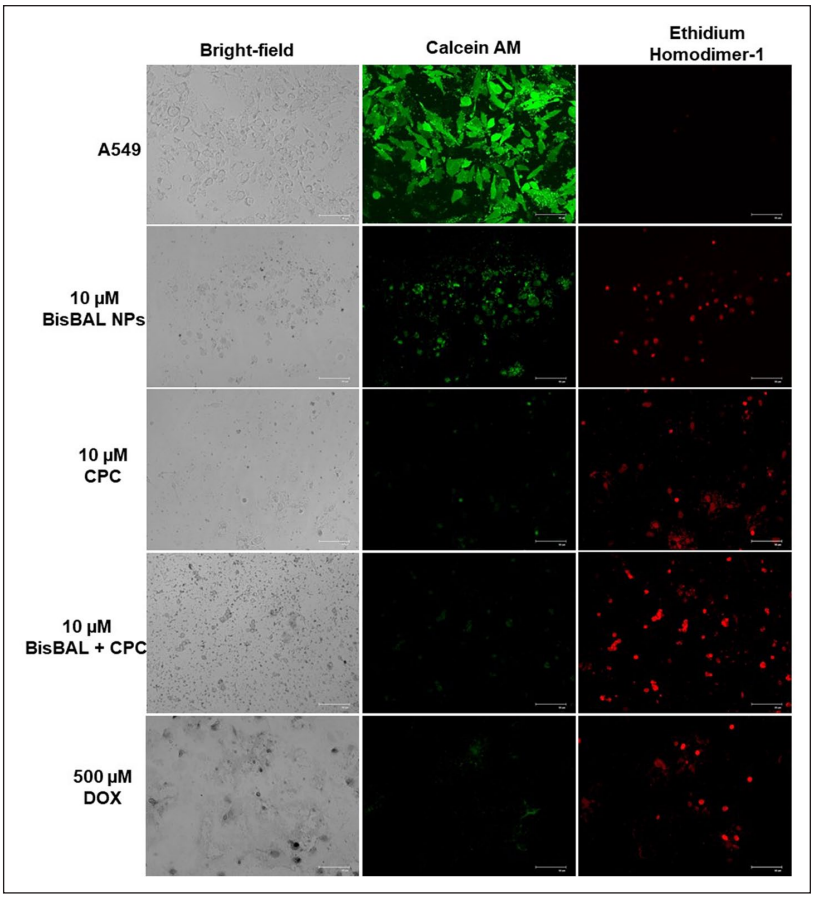

Figure 3. Drug cytotoxicity on lung tumor cells. The effect of 10 µM CPC, 10 µM BisBAL NP, a 10 µM 1:1 CPC-BisBAL NP mixture, and 500 µM doxorubicin (DOX; positive control of cytotoxicity) on A549 cells was analyzed by bright-field and LIVE/DEAD assays after a 24-h exposure. Bar, 125 µm.

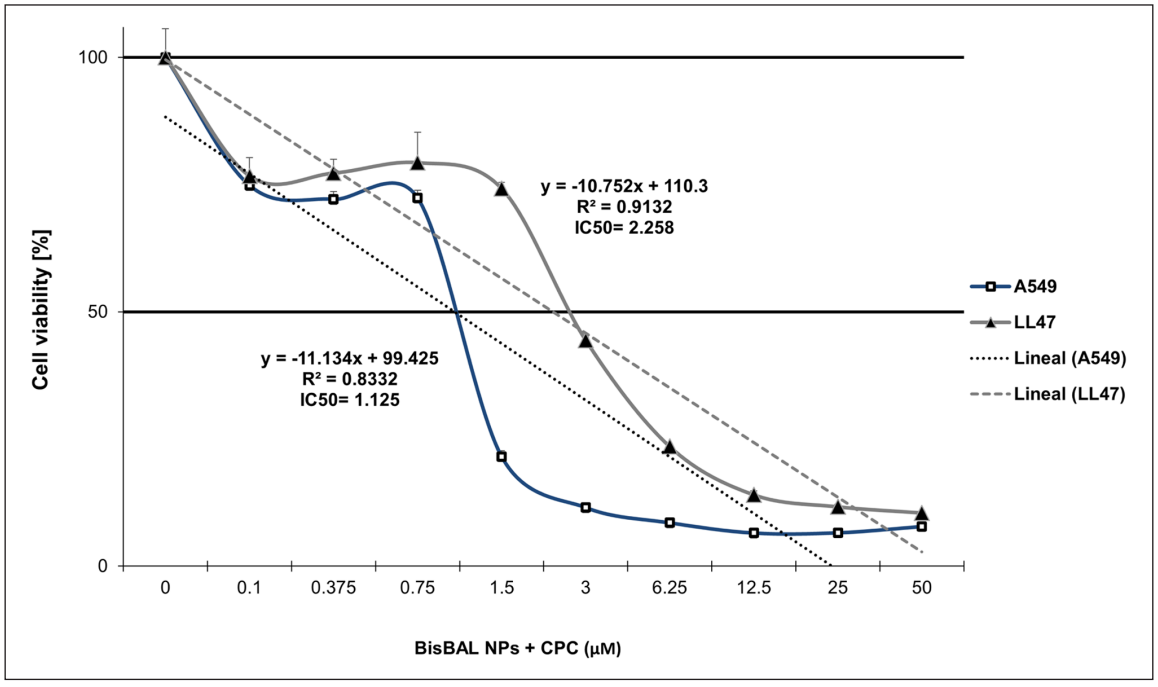

Figure 4. IC_{50} value of BisBAL NP/CPC on A549 and LL47(MaDo) cells. A549 and LL47(MaDo) cells were exposed for 24 h to a concentration series of BisBAL NP/CPC (0.1, 0.375, 0.75, 1.5, 3, 6.25, 12.5, 25, and 50 µM), mixed 1:1; followed by a viability assay to determine the IC_{50}. Three independent experiments were done in triplicate.

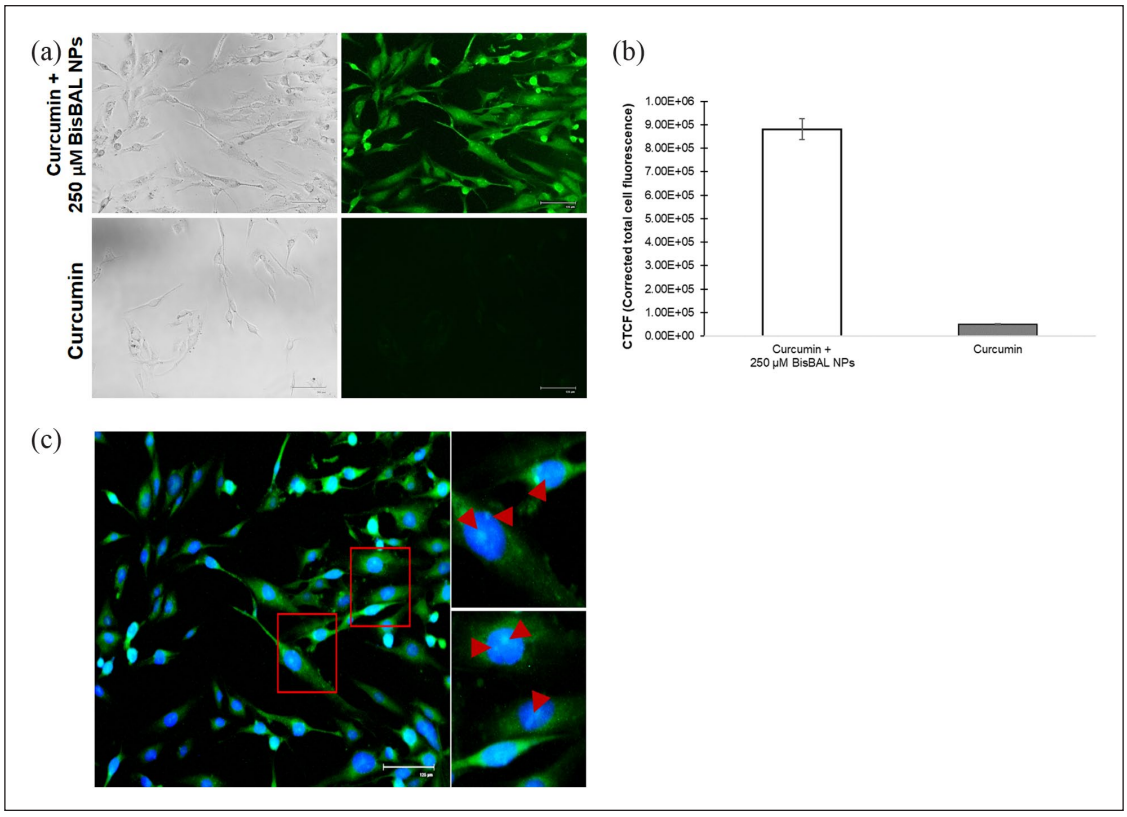

Figure 5. BisBAL NP-Cur uptake by A549 cells: (a) 250 µM BisBAL NP was mixed with 4 µL of a curcumin solution. A549 cells were exposed for 30 min–2 h to conjugate BisBAL NP-Cur at 37°C in the dark, (b) after a triple wash in phosphate-buffered saline solution, cells were observed with an EVOS Cell Imaging System (Thermo Fisher Scientific, CA, USA) using a FITC filter. Bar, 60 µm, and (c) similar to (a), but an additional DAPI stain and a higher zoom during observation. Bar, 125 µm. Square and arrows indicate BisBAL NP-Cur localization inside cells and nuclei.

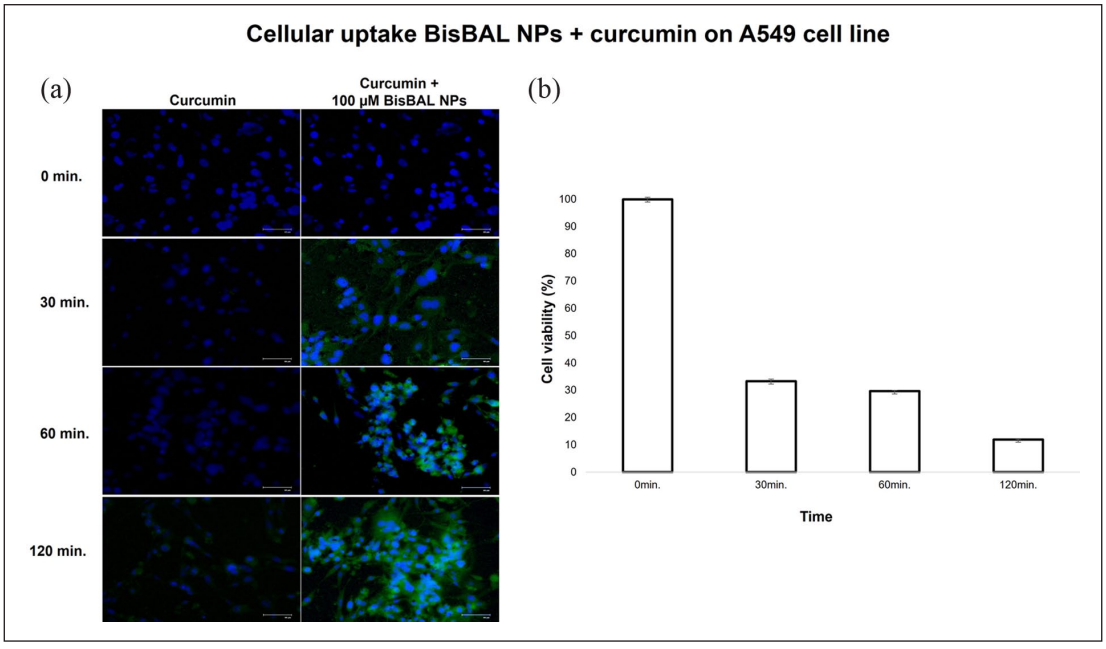

Figure 6. BisBAL NP entry into A549 cells at different exposure times. BisBAL NP (100 µM) was labeled with curcumin and A549 cells were exposed to the BisBAL NP-Cur conjugate for 30, 60, or 120 min at 37°C in the dark: (a) after a triple PBS wash, cells were observed with an EVOS Cell Imaging System (Thermo Fisher Scientific, CA, USA) using a FITC filter. Bar, 60 µm and (b) cell viability according to the Prestoblue assay at the indicated exposure times.

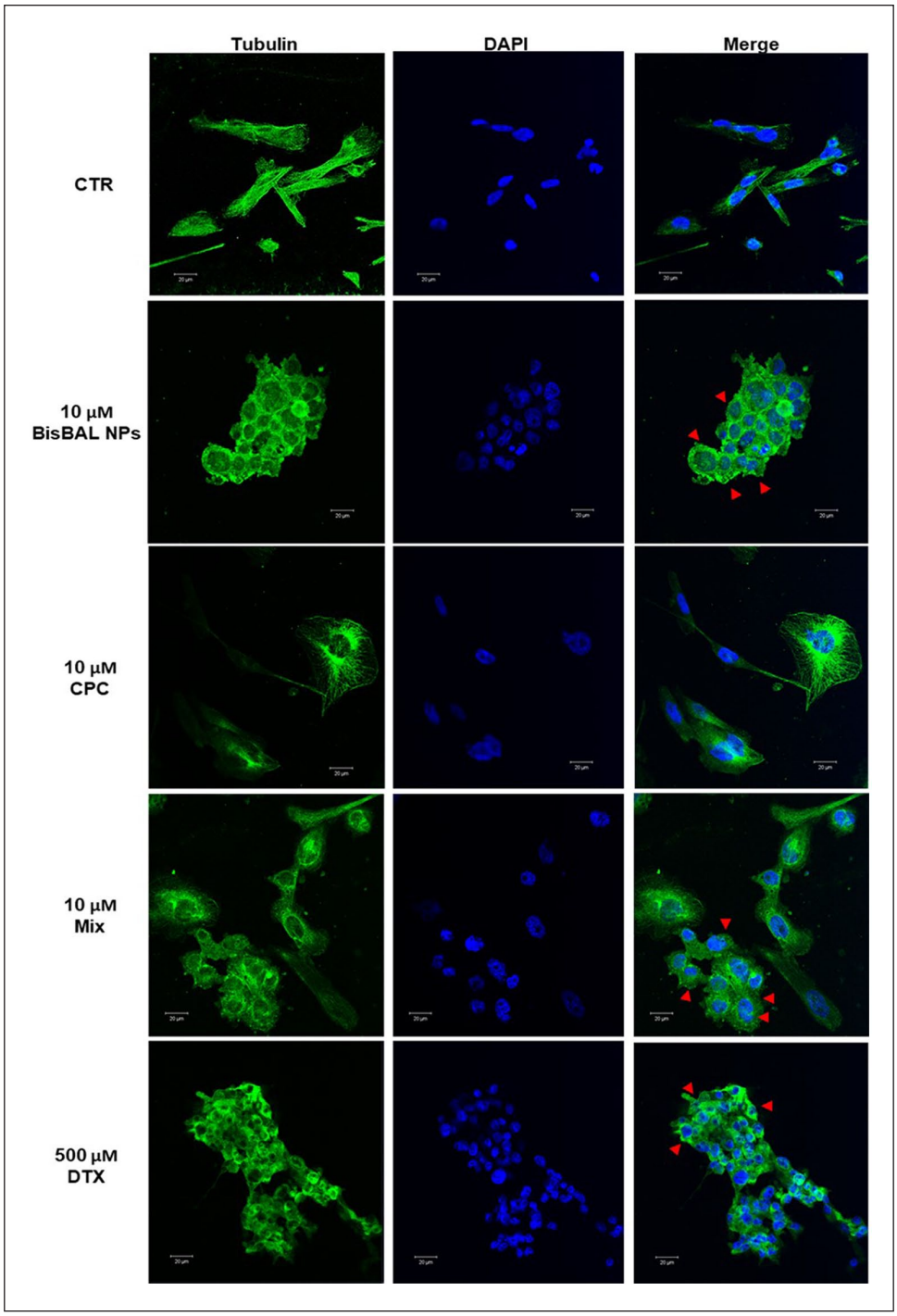

Figure 7. Tubulin immunoreactivity within A549 cells after a 24-h exposure to BisBAL NP, CPC, or the BisBAL NP/CPC mixture. A549 cells were exposed for 24 h to 10 μM BisBAL NP, 10 μM CPC, 10 μM 1:1 BisBAL NP/CPC mixture, or 500 μM DTX as a positive control of inhibition. Drug-free cultures served as growth controls (CTR). Green, tubulin immunoreactivity (AB-197737; Abcam, Cambridge, UK); blue, nuclei (DAPI; 100 μL/well). A confocal microscope, using FITC and DAPI filters (Zeiss LSM 7 Duo; Carl Zeiss; Germany), was used for observation.

susceptible than normal healthy cells. It has been reported that the lipophilic and cationic character of BisBAL NP increase the affinity for human breast cancer cells.[17] The anti-tumor activity of paclitaxel also increased when it was combined with solid lipid nanoparticles and curcumin.[34] As far as we know, the current study is the first to report on combination therapies of anti-tumor drugs with CPC on human LC cells.

Through curcumin-labeling and uptake assays we corroborated that BisBAL NP were effectively internalized into tumor cells, as previous studies suggested.[35,36] Yin et al.[37] described the internalization of curcumin-loaded IRMOF-10 nanoparticles after a 30-min exposure. BisBAL NP internalization into A549 cells also occurred within 30 min and augmented with time, which correlated with timelines of more severe growth inhibition. Interestingly, intracellular BisBAL NP-Cur localized preferably within the nuclei, which is consistent with BisBAL NP-induced genotoxicity on human breast cancer cells.[17] Besides, both BisBAL NP and CPC have been reported to alter membrane permeability and promote lysis of cancer cells.[17,22] Results from the current study suggest that cytoplasmic BisBAL NP may also interfere with the microtubule network of A549 cells as does the antitumor drug DTX. It is well known that the cytotoxicity of DTX is achieved through inhibition of microtubule dynamics.[38,39] Based on the similar tubulin immunoreactivity profiles of A549 cells after exposure to DTX and BisBAL NP, we hypothesize that BisBAL NP may interfere with the microtubule network and interrupt the cell cycle, like DTX does. Cytoskeletal alterations have also been reported in tumor cells and macrophages that had been exposed for 2-to-3-days to iron oxide nanoparticles.[40] It may be interesting to know whether other cytoskeleton elements, like actin and intermediate filaments, are also affected by BisBAL NP exposure.

In summary, this study presents evidence of the antitumor effect against the A549 human LC cell line after exposure to BisBAL NP and CPC individually or in combination, as of 1 µM. The BisBAL NP/CPC combination has a cumulative effect compared to individual exposure, which can be explained by their different and complementary modes of action. BisBAL NP affects microtubule organization in a manner similar to DTX, while CPC does not have this effect. BisBAL NP was taken up by A549 cells within 30 min and was correlated with a decrease in cell growth.

Conclusions

The combination of BisBAL NP and CPC inhibited A549 cell growth as of 1 µM. The mixture of BisBAL NP and CPC constitutes an innovative low-cost alternative to treat human LC.

Declaration of conflicting interests

The author(s) declared no potential conflicts of interest with respect to the research, authorship, and/or publication of this article.

Funding

The author(s) disclosed receipt of the following financial support for the research, authorship, and/or publication of this article: The authors want to thank the CONACyT for the Sectorial Fund for Education Research, Ciencia de Frontera 2023. Instituto Nacional de Cancerología – INCan Mexico, RAI, UNAM – Advanced Microscopy Applications Unit (ADMiRA), RRID: SCR_022788.

ORCID iDs

Jesús Alejandro Torres-Betancourt https://orcid.org/0000-0002-9873-7603

Nayely Pineda-Aguilar https://orcid.org/0000-0002-3894-597X

Claudio Cabral-Romero https://orcid.org/0000-0002-2657-0111

References

1. Ramalingam SS, Owonikoko TK and Khuri FR. Lung cancer: new biological insights and recent therapeutic advances. *CA Cancer J Clin* 2011; 61: 91–112.
2. Ferlay J, Colombet M, Soerjomataram I, et al. Cancer statistics for the year 2020: an overview. *Int J Cancer*. Epub ahead of print 5 April 2021. DOI: 10.1002/ijc.33588.
3. Siegel RL, Miller KD and Jemal A. Cancer statistics, 2019. *CA Cancer J Clin* 2019; 69: 7–34.
4. Aldaco-Sarvide F, Pérez-Pérez P, Cervantes-Sánchez MG, et al. Mortalidad por cáncer en México: actualización 2015. *Gaceta Mexicana de Oncología* 2018; 17: 28–34.
5. Zhong L, Goldberg MS, Parent ME and Hanley JA. Exposure to environmental tobacco smoke and the risk of lung cancer: a meta-analysis. *Lung Cancer* 2000; 27: 3–18.
6. Bruce N, Dherani M, Liu R, et al. Does household use of biomass fuel cause lung cancer? A systematic review and evaluation of the evidence for the GBD 2010 study. *Thorax* 2015; 70: 433–441.
7. Ecologia. Secretariat for Natural Resources and the Environment and National Institute for Ecology. *Fourth database of data regarding trends in air quality for 20 Mexican cities (2000–2009)*. inecc.gob.mx/archivo/informes/3erAlmanaque.pdf (2018, accessed 20 December 2018).
8. Hussain S. Nanomedicine for treatment of lung cancer. *Adv Exp Med Biol* 2016; 890: 137–147.
9. Podyacheva E and Toropova Y. SIRT1 activation and its effect on intercalated disc proteins as a way to reduce doxorubicin cardiotoxicity. *Front Pharmacol* 2022; 13: 1035387.
10. Injac R and Strukelj B. Recent advances in protection against doxorubicin-induced toxicity. *Technol Cancer Res Treat* 2008; 7: 497–516.
11. Paz MM and Champeil E. Insight into factors governing formation, synthesis and stereochemical configuration of DNA adducts formed by mitomycins. *Chem Rec* 2023; 23: e202200193.
12. Heigener DF and Reck M. Crizotinib. *Recent Results Cancer Res* 2018; 211: 57–65.
13. Abdelgalil AA, Al-Kahtani HM and Al-Jenoobi FI. Erlotinib. *Profiles Drug Subst Excip Relat Methodol* 2020; 45: 93–117.
14. Hosomi Y, Morita S, Sugawara S, et al. Gefitinib alone versus Gefitinib plus chemotherapy for non-small-cell lung cancer with mutated epidermal growth factor receptor: NEJ009 study. *J Clin Oncol* 2020; 38: 115–123.
15. Nguyen PV, Hervé-Aubert K, Lajoie L, et al. In vitro synergistic activity of cisplatin and EGFR-targeted nanomedicine of anti-Bcl-xL siRNA in a non-small lung cancer cell line model. *Int J Pharm* 2022; 4: 122335.

16. Wang YJ, Wang J, Hao DL, et al. [Preparation of docetaxel-loaded nanomicelles and their anti-Lewis lung cancer effect in vitro]. *Zhongguo Zhong Yao Za Zhi* 2019; 44: 2251–2259.
17. Hernandez-Delgadillo R, García-Cuéllar CM, Sánchez-Pérez Y, et al. In vitro evaluation of the antitumor effect of bismuth lipophilic nanoparticles (BisBAL NPs) on breast cancer cells. *Int J Nanomedicine* 2018; 13: 6089–6097.
18. Cabral-Romero C, Solís-Soto JM, Sánchez-Pérez Y, et al. Antitumor activity of a hydrogel loaded with lipophilic bismuth nanoparticles on cervical, prostate, and colon human cancer cells. *Anticancer Drugs* 2020; 31: 251–259.
19. Martínez-Pérez F, García-Cuellar CM, Hernandez-Delgadillo R, et al. Comparative study of antitumor activity between lipophilic bismuth nanoparticles (BisBAL NPs) and chlorhexidine on human squamous cell carcinoma. *J Nanomat* 2019; 2019: 8148219.
20. Mao X, Auer DL, Buchalla W, et al. Cetylpyridinium chloride: mechanism of action, antimicrobial efficacy in biofilms, and potential risks of resistance. *Antimicrob Agents Chemother* 2020; 64: e00576-20.
21. Allen SA, Datta S, Sandoval J, et al. Cetylpyridinium chloride is a potent AMP-activated kinase (AMPK) inducer and has therapeutic potential in cancer. *Mitochondrion* 2020; 50: 19–24.
22. García-Cuellar CM, Hernández-Delgadillo R, Solis-Soto JM, et al. Cetylpyridinium chloride inhibits human breast tumor cells growth in a no-selective way. *J Appl Biomater Funct Mater* 2022; 20: 22808000221092157.
23. Kim H, Yoo J, Lim YM, et al. Comprehensive pulmonary toxicity assessment of cetylpyridinium chloride using A549 cells and Sprague-Dawley rats. *J Appl Toxicol* 2021; 41: 470–482.
24. Badireddy AR, Hernandez-Delgadillo R, Sánchez-Nájera RI, Chellam S and Cabral-Romero C. Synthesis and characterization of lipophilic bismuth dimercaptopropanol nanoparticles and their effects on oral microorganisms growth and biofilm formation. *J Nanopart Res* 2014; 16: 2456.
25. Xu M, McCanna DJ and Sivak JG. Use of the viability reagent PrestoBlue in comparison with alamarblue and MTT to assess the viability of human corneal epithelial cells. *J Pharmacol Toxicol Methods* 2015; 71: 1–7.
26. Gonzalez TL, Hancock M, Sun S, et al. Targeted degradation of activating estrogen receptor α ligand-binding domain mutations in human breast cancer. *Breast Cancer Res Treat* 2020; 180: 611–622.
27. Mazarei M, Mohammadi Arvejeh P, Mozafari MR, Khosravian P and Ghasemi S. Anticancer potential of temozolomide-loaded eudragit-chitosan coated selenium nanoparticles: in vitro evaluation of cytotoxicity, apoptosis and gene regulation. *Nanomater* 2021; 11: 1704.
28. Jurczyk M, Kasperczyk J, Wrześniok D, Beberok A and Jelonek K. Nanoparticles loaded with docetaxel and resveratrol as an advanced tool for cancer therapy. *Biomedicines* 2022; 10: 1187.
29. Darvish M, Nasrabadi N, Fotovat F, et al. Biosynthesis of Zn-doped $CuFe_2O_4$ nanoparticles and their cytotoxic activity. *Sci Rep* 2022; 12: 9442.
30. Skóra B, Piechowiak T and Szychowski KA. Epidermal growth factor-labeled liposomes as a way to target the toxicity of silver nanoparticles into EGFR-overexpressing cancer cells in vitro. *Toxicol Appl Pharmacol* 2022; 443: 116009.
31. Lee TH, Chen HL, Chang HM, et al. Impact of smoking status in combination treatment with EGFR tyrosine kinase inhibitors and anti-angiogenic agents in advanced non-small cell lung cancer harboring susceptible EGFR mutations: systematic review and meta-analysis. *J Clin Med* 2022; 11: 3366.
32. Fu B, Dou X, Zou M, et al. Anticancer effects of amlodipine alone or in combination with gefitinib in non-small cell lung cancer. *Front Pharmacol* 2022; 13: 902305.
33. Norouzi M, Yathindranath V, Thliveris JA, Kopec BM, Siahaan TJ and Miller DW. Doxorubicin-loaded iron oxide nanoparticles for glioblastoma therapy: a combinational approach for enhanced delivery of nanoparticles. *Sci Rep* 2020; 10: 11292.
34. Pi C, Zhao W, Zeng M, et al. Anti-lung cancer effect of paclitaxel solid lipid nanoparticles delivery system with curcumin as co-loading partner in vitro and in vivo. *Drug Deliv* 2022; 29: 1878–1891.
35. Del Prado-Audelo ML, Magaña JJ, Mejía-Contreras BA, et al. In vitro cell uptake evaluation of curcumin-loaded PCL/F68 nanoparticles for potential application in neuronal diseases. *J Drug Deliv Sci Tech* 2019; 52: 905–914.
36. Stati G, Rossi F, Trakoolwilaiwan T, et al. Development and characterization of curcumin-silver nanoparticles as a promising formulation to test on human pterygium-derived keratinocytes. *Molecules* 2022; 27: 282.
37. Yin D, Hu X, Cai M, et al. Preparation, characterization, and in vitro release of curcumin-loaded IRMOF-10 nanoparticles and investigation of their pro-apoptotic effects on human hepatoma HepG2 cells. *Molecules* 2022; 27: 3940.
38. Antonarakis ES and Armstrong AJ. Evolving standards in the treatment of docetaxel-refractory castration-resistant prostate cancer. *Prostate Cancer Prostatic Dis* 2011; 14: 192–205.
39. Farha NG and Kasi A. Docetaxel. *StatPearls*. Treasure Island, FL: StatPearls Publishing LLC, 2022.
40. Janik-Olchawa N, Drozdz A, Ryszawy D, et al. The influence of IONPs core size on their biocompatibility and activity in in vitro cellular models. *Sci Rep* 2021; 11: 21808.